⌘ *Author's Choice*

THE JOURNAL OF BIOLOGICAL CHEMISTRY VOL. 287, NO. 44, pp. 36990–36998, October 26, 2012

Structure of the Bone Morphogenetic Protein Receptor ALK2 and Implications for Fibrodysplasia Ossificans Progressiva*[S]

Received for publication, March 23, 2012, and in revised form, August 28, 2012 Published, JBC Papers in Press, September 12, 2012, DOI 10.1074/jbc.M112.365932

Apirat Chaikuad[‡1], Ivan Alfano[‡1], Georgina Kerr[‡1], Caroline E. Sanvitale[‡], Jan H. Boergermann[§], James T. Triffitt[¶], Frank von Delft[‡], Stefan Knapp[‡], Petra Knaus[§], and Alex N. Bullock[‡2]

From the [‡]Structural Genomics Consortium, University of Oxford, Oxford OX3 7DQ, United Kingdom, the [§]Institute for Chemistry/Biochemistry, Freie Universität Berlin, Berlin 14195, Germany, and the [¶]Botnar Research Centre, University of Oxford, Oxford OX3 7LD, United Kingdom

Background: Mutations in the ALK2 kinase cause extraskeletal bone formation.
Results: We solved the structure of ALK2 in complex with the inhibitor FKBP12.
Conclusion: Disease mutations break critical interactions that stabilize the inactive ALK2-FKBP12 complex leading to kinase activation.
Significance: We offer an explanation for the effects of mutation and a structural template for the design of small molecule inhibitors.

Bone morphogenetic protein (BMP) receptor kinases are tightly regulated to control development and tissue homeostasis. Mutant receptor kinase domains escape regulation leading to severely degenerative diseases and represent an important therapeutic target. Fibrodysplasia ossificans progressiva (FOP) is a rare but devastating disorder of extraskeletal bone formation. FOP-associated mutations in the BMP receptor ALK2 reduce binding of the inhibitor FKBP12 and promote leaky signaling in the absence of ligand. To establish structural mechanisms of receptor regulation and to address the effects of FOP mutation, we determined the crystal structure of the cytoplasmic domain of ALK2 in complex with the inhibitors FKBP12 and dorsomorphin. FOP mutations break critical interactions that stabilize the inactive state of the kinase, thereby facilitating structural rearrangements that diminish FKBP12 binding and promote the correct positioning of the glycine-serine-rich loop and αC helix for kinase activation. The balance of these effects accounts for the comparable activity of R206H and L196P. Kinase activation in the clinically benign mutant L196P is far weaker than R206H but yields equivalent signals due to the stronger interaction of FKBP12 with R206H. The presented ALK2 structure offers a valuable template for the further design of specific inhibitors of BMP signaling.

Bone morphogenetic proteins (BMPs)[3] are members of the transforming growth factor-β (TGF-β) superfamily determining embryonic patterning and tissue morphogenesis (1–3). These dimeric ligands induce intracellular signaling by binding to a unique family of transmembrane receptor serine/threonine kinases that assemble as heteromeric complexes consisting of two type II and two type I receptors. Type II receptors are required to activate the type I receptors by phosphorylation of their juxtamembrane glycine-serine-rich (GS) domain (4). Activated type I receptors then phosphorylate receptor-associated Smads (R-Smads), which subsequently assemble with Smad4 (Co-Smad) for nuclear transport and transcriptional activation (5). Other pathways activated include the p38 MAPK family (6).

Five different type II receptors and seven type I receptors (also known as activin receptor-like kinases, ALK1–7) are identified in mammals. The type II receptors show constitutive activity, demanding strict control of the substrate GS domain. Structures of the type I TGF-β receptor ALK5 (TβR-I) show that FKBP12 (the 12-kDa FK506-binding protein) competes for binding to the GS domain and thereby inhibits leaky activation in the absence of ligand (7, 8). Ligand induces a phosphorylation-dependent switch in the GS domain that dissociates FKBP12 and facilitates docking of the R-Smad MH2 domain (9). Structures of the R-Smad identify a Ser(P)-Xaa-Ser(P)-binding module closely related to the Forkhead associated domain of forkhead transcription factors (10, 11).

BMP signaling is dysregulated in the rare but devastating bone disease fibrodysplasia ossificans progressiva (FOP) (12). From early childhood, affected individuals suffer progressive ectopic bone formation in skeletal muscle and connective tissue that ultimately renders movement impossible. The effects of FOP are accelerated by inflammation and trauma, precluding surgical intervention, and there is an urgent need for an effective treatment (13). Linkage analysis led to the identification of a recurrent heterozygous mutation (617G → A; R206H) in the type I BMP receptor ALK2 (*ACVR1*) (14). Additional FOP mutations have since been identified in both the GS and kinase domains of ALK2 that differentially affect the age of onset of

* This work was supported in part by a Roemex postdoctoral fellowship (to G. K.), the University of Oxford FOP Research Fund (to C. E. S.), and German Research Foundation Collaborative Research Centre Grant SFB 760 (to P. K.).
⌘ *Author's Choice*—Final version full access.
[S] This article contains supplemental Fig. S1.
The atomic coordinates and structure factors (code 3H9R) have been deposited in the Protein Data Bank (http://wwpdb.org/).
[1] These authors contributed equally to this work.
[2] To whom correspondence should be addressed. Tel.: 44 1865 617754; Fax: 44 1865 617575; E-mail: alex.bullock@sgc.ox.ac.uk.
[3] The abbreviations used are: BMP, bone morphogenetic protein; FOP, fibrodysplasia ossificans progressiva; GS, glycine-serine-rich; BisTris, 2-[bis(2-hydroxyethyl)amino]-2-(hydroxymethyl)propane-1,3-diol; BRE, BMP-response element.

ossification, as well as the extent of skeletal malformation (15–20).

The FOP condition is recapitulated in animal models by transgenic overexpression of BMP4 (21) or caALK2 (22), a classic constitutively active ALK2 receptor containing the artificial mutation Q207D (23). Both proteins can induce osteogenic differentiation in mesenchymal progenitor cells, potentially explaining the origin of heterotopic ossification in FOP (24). Analyses of a subset of ALK2 FOP mutants, including L196P, R206H, and G356D, suggest that FOP mutations are more weakly activating than caALK2 but show similar potential to induce osteogenic differentiation through reduced FKBP12 binding and increased Smad1/5/8 phosphorylation (25–30).

The recent discovery of dorsomorphin, the first chemical inhibitor of BMP receptor signaling, provides hope for future FOP therapies (31). Indeed, the more potent derivative LDN-193189 reduced the effects of FOP in a mouse model expressing caALK2 (22). Both compounds inhibit BMP-induced phosphorylation of Smad1/5/8 but not the TGF-β-induced phosphorylation of Smad2/3.

Here, we investigated a large panel of FOP mutants affecting both the GS and kinase domains to compare their relative activation and sensitivity to FKBP12. To further understand the molecular basis for these effects, we determined the crystal structure of ALK2 in complex with FKBP12 and dorsomorphin. All FOP mutations are predicted to destabilize the inactive receptor conformation promoting a shift toward kinase activation.

EXPERIMENTAL PROCEDURES

Expression Vectors—Constructs were prepared by ligation-independent cloning. Full-length human FKBP12 (Uniprot ID, P62942) was cloned into pNIC28-Bsa4 for bacterial expression. The GS and kinase domains of ALK2 (residues 172–499; Uniprot ID, Q04771) were cloned into pFB-LIC-Bse for baculoviral expression. Full-length human ALK2 was cloned into pcDNA3.1, and mutations were engineered using the QuikChange site-directed mutagenesis kit (Stratagene). HA-FKBP12 plasmid was a gift of C. R. Bertozzi (Addgene plasmid 20220). All constructs were verified by sequencing.

Luciferase Reporter Gene Assay—C2C12 cells were co-transfected using Lipofectamine 2000 with BRE-luciferase (51), *Renilla* luciferase pRLTK (Promega), and the indicated ALK2 constructs, following the manufacturer's instructions. 16 h after transfection, cells were starved for 7 h in DMEM containing 1% FCS. Cells were then incubated overnight untreated or treated with 1 μM FK506 or 10 ng/ml BMP4 or 50 ng/ml BMP6 before lysis. Luciferase activities were determined according to the Dual-Luciferase® reporter assay system (Promega) using *Renilla* for normalization of transfection efficiency. Results are the means ± S.E. of at least three independent experiments, each performed in triplicate. Statistical analyses for determination of p values used the Student's t test. $p < 0.05$ was considered significant.

Immunoprecipitation—C2C12 or HEK293 cells were transfected with FLAG-tagged ALK2 and HA-tagged FKBP12 by FuGENE (Promega), following the manufacturer's protocol. The following day, cells were lysed for 1 h at 4 °C in buffer containing 150 mM NaCl, 20 mM Tris-HCl, pH 7.5, 0.1% Triton X-100, and protease inhibitors (Roche Applied Science). Lysates were clarified by centrifugation, and the protein concentration was measured using the BCA assay (Pierce). 1 mg of lysate was incubated with anti-HA-agarose beads (Sigma) for 2 h at 4 °C before the beads were washed thoroughly in lysis buffer and resuspended in 20 μl of SDS-PAGE loading dye. Samples were run on a 4–12% BisTris pre-cast gel (Criterion), transferred onto PVDF or nitrocellulose (GE Healthcare) and probed with the relevant antibody; anti-FLAG-HRP (Sigma), or anti-HA (12CA5, Roche Applied Science). Bands were detected by ECL (Pierce) and images acquired on a LAS-4000 image analyzer. Band intensities were quantified using the Kodak ID program.

Protein Expression—The FKBP12 plasmid was transformed into *Escherichia coli* strain BL21(DE3)R3-pRARE2 for expression. Cultures in LB media were induced with 0.5 mM isopropyl 1-thio-β-D-galactopyranoside overnight at 18 °C, and the cells were harvested and lysed by ultrasonication. ALK2 was expressed in Sf9 insect cells grown at 27 °C. Some 48 h post-infection, cells were harvested and lysed using a C5 high pressure homogenizer (Emulsiflex). Both proteins were initially purified separately by nickel affinity chromatography. The ALK2-FKBP12 complex was prepared by size exclusion chromatography mixing an excess of FKBP12. The eluted complex was stored in 50 mM HEPES, pH 7.5, 150 mM NaCl, 10 mM DTT. The hexahistidine tags of ALK2 and FKBP12 were cleaved using tobacco etch virus protease.

Crystallization—Crystallization was achieved at 4 °C using the sitting-drop vapor diffusion method. The ALK2-FKBP12 complex was preincubated with 1 mM dorsomorphin (Calbiochem) at a protein concentration of 10 mg/ml and crystallized using a precipitant containing 30% PEG3350, 0.25 M ammonium sulfate, and 0.1 M BisTris, pH 6.0. Viable crystals were obtained when the protein solution was mixed with the reservoir solution at 2:1 volume ratio. Crystals were cryoprotected with mother liquor plus 20% PEG400, prior to vitrification in liquid nitrogen.

Data Collection—Diffraction data were collected at the Diamond Light Source, station I02 using monochromatic radiation at wavelength 0.9050 Å.

Phasing, Model Building, Refinement, and Validation—Data were processed with MOSFLM (32) and subsequently scaled using the program SCALA from the CCP4 suite (33). Initial phases were obtained by molecular replacement using the program PHASER (34) and the structures of FKBP12 (Protein Data Bank code 1A7X) and ALK5 (Protein Data Bank code 1B6C) as search models. Density modification and NCS averaging were performed using the program DM (35), and the improved phases were used in automated model building with the program ARP/wARP (36) and Buccaneer (37). The resulting structure solution was refined using REFMAC5 from the CCP4 suite (38) and manually rebuilt with COOT (39). Appropriate TLS restrained refinement using the tls tensor files calculated from the program TLSMD (40) was applied at the final round of refinement. The complete structure was verified for geometric correctness with MolProbity (41). Data collection and refinement statistics are shown in Table 1.

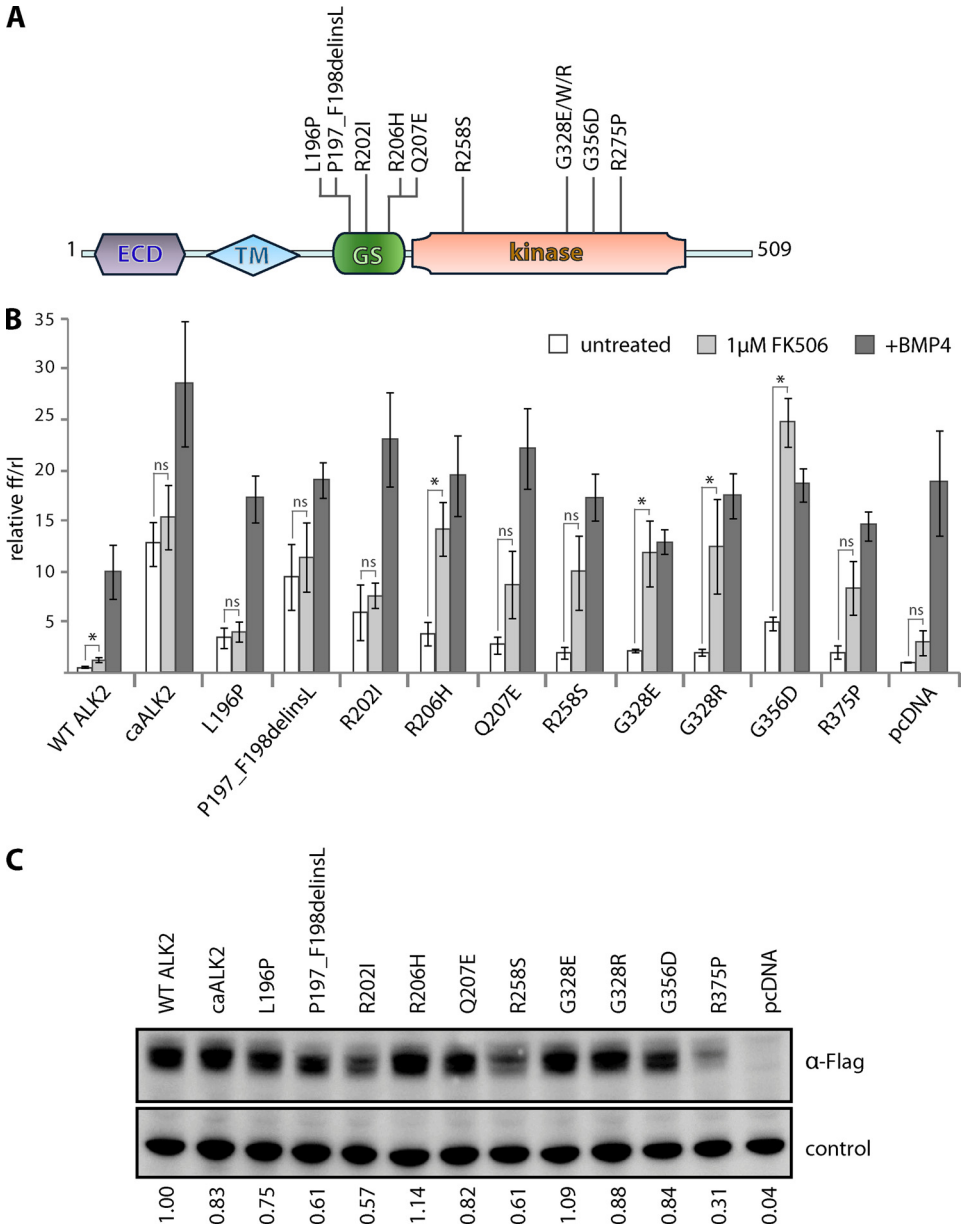

FIGURE 1. **FOP mutations induce gain of function.** *A*, schematic representation of the ALK2 protein showing the domain organization. FOP mutations map to the cytoplasmic GS and kinase domains. *B*, BRE-luciferase reporter assay for constitutive ALK2 activity. C2C12 cells were either left untreated (*white bars*), treated with 1 μM FK506 (*light gray bars*), or 10 ng/ml BMP4 (*dark gray bars*). *y* axis displays the ratio of Firefly/*Renilla* activity for transfected ALK2 constructs relative to vector control. *Error bars* represent standard error of at least three independent experiments performed in triplicate. In comparison with the untreated cells, FK506 significantly enhanced signaling by WT, R206H, G328E, G328R, and G356D (*asterisk* indicates significance at $p < 0.05$), whereas L196P, P197_F198delinsL, R202I, and Q207D were little affected ($p > 0.6$; *ns* indicates not significant). The remaining samples had intermediate *p* values (R258S and R375P were $p < 0.1$). Statistical analyses indicated no significant difference between FK506-treated FOP mutant samples and untreated caALK2 (*p* values >0.1). Additional data determined in parallel for BMP6 are shown in supplemental Fig. S1. *C*, representative expression levels for transfected ALK2 constructs. *Control* represents an endogenous protein bound by the anti-FLAG antibody. *Numbers* below indicate the band intensities for anti-FLAG normalized to control and shown relative to wild type.

RESULTS

FOP Mutants Show Gain of Function—To investigate the effects of FOP mutation (Fig. 1*A*), we tested the functional consequences of these receptors in a Smad-dependent luciferase reporter assay. For this, a BRE-luciferase construct was co-transfected with indicated receptor constructs in C2C12 cells. Signaling from the wild-type ALK2 receptor was observed only upon stimulation with BMP4 (Fig. 1*B*) or BMP6 (supplemental Fig. S1), whereas the activity of the artificial constitutively active mutant caALK2 was induced independently of added ligand (Fig. 1*B*). In comparison, the basal activity of FOP mutants was more moderate, demonstrating that their gain of function was weaker (Fig. 1*B*, *white bars*). Overall, BMP6 signaling was strongly enhanced by ALK2 transfection, consistent with its preferential signaling through this receptor (supplemental Fig. S1) (42, 43). In contrast, BMP4 signaling was lower in wild-type ALK2-transfected cells than the vector control (Fig. 1*B*). We speculate that there is some competitive interference of ALK2 with the preferred endogenous BMP4 receptors ALK3 (BMPR1A) and ALK6 (BMPR1B).

The most active FOP mutant contained a deletion in the GS domain, replacing Pro-197/Phe-198 with a single leucine residue that removes part of the FKBP12 interaction site. To assess whether the activity of other FOP mutants was generally restricted by endogenous FKBP12, we treated the cells with the FKBP12 ligand FK506 (also known as the immunosuppressant Tacrolimus). FK506 competes with the GS domain for binding to FKBP12 and thereby dissociates FKBP12 from receptors (44). Under these conditions, the signaling from the wild-type receptor was increased 2.5-fold (Fig. 1*B*, *light gray bars*) but remained relatively low, indicating that the mechanism of activation in FOP extends beyond the simple disruption of FKBP12 binding. In comparison, the activity of some FOP mutants was generally increased to a level similar to caALK2, revealing an inherent gain of function in their catalytic domain in the absence of added BMP ligand (Fig. 1*B*). Significantly, the signaling by R206H was increased by FK506 to a far greater extent than other GS domain mutants, such as L196P (Fig. 1*B*).

The different responses of L196P and R206H to FK506 may be explained by their different affinities for FKBP12. To test this hypothesis, we transiently co-transfected HA-tagged FKBP12 with wild type, L196P, and R206H ALK2 constructs into C2C12 cells and performed an HA immunoprecipitation. In agreement with their responses to FK506 in the luciferase reporter assay, wild-type ALK2 and the R206H mutant showed significant binding to FKBP12, whereas the interaction of L196P was essentially lost (Fig. 2*A*). All FKBP12 interactions were inhibited by FK506 (Fig. 2*A*). Similar results were obtained in HEK293 cells (Fig. 2*B*), although under less saturating conditions the FKBP12 binding of R206H was notably weaker than wild type. Together, the BRE-luciferase and immunoprecipitation data suggest that FKBP12 remains an important modulator of receptor function in the majority of FOP cases where mutations fall outside the core FKBP12-binding site.

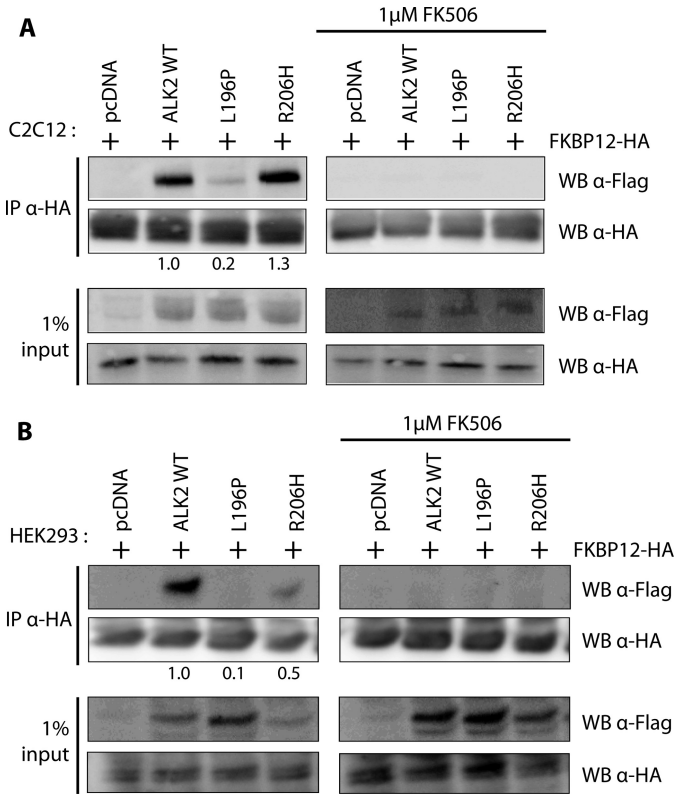

FIGURE 2. **FOP mutations reduce FKBP12 binding.** *A*, immunoprecipitation (*IP*) to determine FKBP12 binding to ALK2 in C2C12 cells transfected with FLAG-tagged ALK2 and HA-tagged FKBP12. Cells were either left untreated or treated with 1 μM FK506 as indicated. Proteins were detected with the indicated antibodies. The amount of immunoprecipitated ALK2 in each lane was quantified, normalized to input, and displayed relative to wild type. *B*, immunoprecipitation to determine FKBP12 binding to ALK2 in HEK293 cells treated as in *A*. *WB*, Western blot.

Overview of the ALK2-FKBP12 Structure—To understand the structural consequences of FOP mutation, we co-purified the cytoplasmic region of ALK2 containing the GS and kinase domains (residues 172–499) with FKBP12 and determined the crystal structure of the complex at 2.35 Å resolution (Fig. 3*A*). Parts of the activation loop (A loop) and L45 loop were disordered and excluded from the model. A summary of statistics for data collection and refinement is reported in Table 1. Overall, ALK2 adopts the typical bilobal kinase architecture with a pattern of specific insertions that define the TGF-β/BMP receptor family (8). These include the L45 loop, the E6 loop, insertions flanking the αF helix, and an insertion in the substrate pocket preceding the αG helix.

The GS domain extends at the start of the N-lobe in a helix-loop-helix motif that binds FKBP12 similarly to ALK5 (8). Binding is dominated by insertion of the αGS2 helix into the central FK506-binding pocket of FKBP12. Here, the ALK5 residues Leu-195–Leu-196 are replaced by ALK2 Phe-198–Leu-199 resulting is a subtle shift in the packing of the interface and the position of FKBP12 (Fig. 3*B*). However, the overall structures of the two complexes are highly conserved (Cα root mean square deviation of 1.5 Å).

The small molecule inhibitor dorsomorphin binds to the ATP-binding pocket with an ATP-mimetic binding mode, while oriented parallel to the hinge (Fig. 3, *A* and *C*). The core pyrazolo[1,5-*a*]pyrimidine ring forms a single hydrogen bond to the hinge amide of His-286. The substituent 4-pyridine ring is accommodated in a hydrophobic pocket formed by Val-222, Leu-263, Leu-281, and Ala-353 and forms a water-mediated hydrogen bond with Glu-248 (αC). On the other side of the inhibitor, the phenyl ring packs below the β1 strand with its plane stacking between Gly-289 and the side chain of Val-214. Further contact is made with the hinge residue Tyr-285, whereas the piperidinyl-ethoxy group is largely extended away into solvent.

Structural Changes Determining Receptor Activation—To understand the structural changes between type I receptors and constitutively active type II receptors, we compared the ALK2 structure with those of the type II activin (ActRIIB) (45) and BMP (BMPRII) receptors (Fig. 4*A*). Superposition shows that the structures are closely matched with the exception of structural elements linked to the activation state of the catalytic domain. The ALK2 structure displays an inhibited conformation of both the GS and kinase domains (Fig. 4*A*). The GS loop is protected from phosphorylation by coordination with Arg-258, which buries the GS loop in the kinase N-lobe between αC and β4 (Fig. 4*B*). As a result, the αC helix is swung away from the catalytic domain at its C terminus and inwards at its N terminus (Fig. 4*A*). This packing is stabilized by the A loop residue Arg-375 that forms inhibitory salt bridges with the catalytic HRD (Asp-336) and DFG (Asp-354) motifs as well as a hydrogen bond to Ser-244 (αC) (Fig.

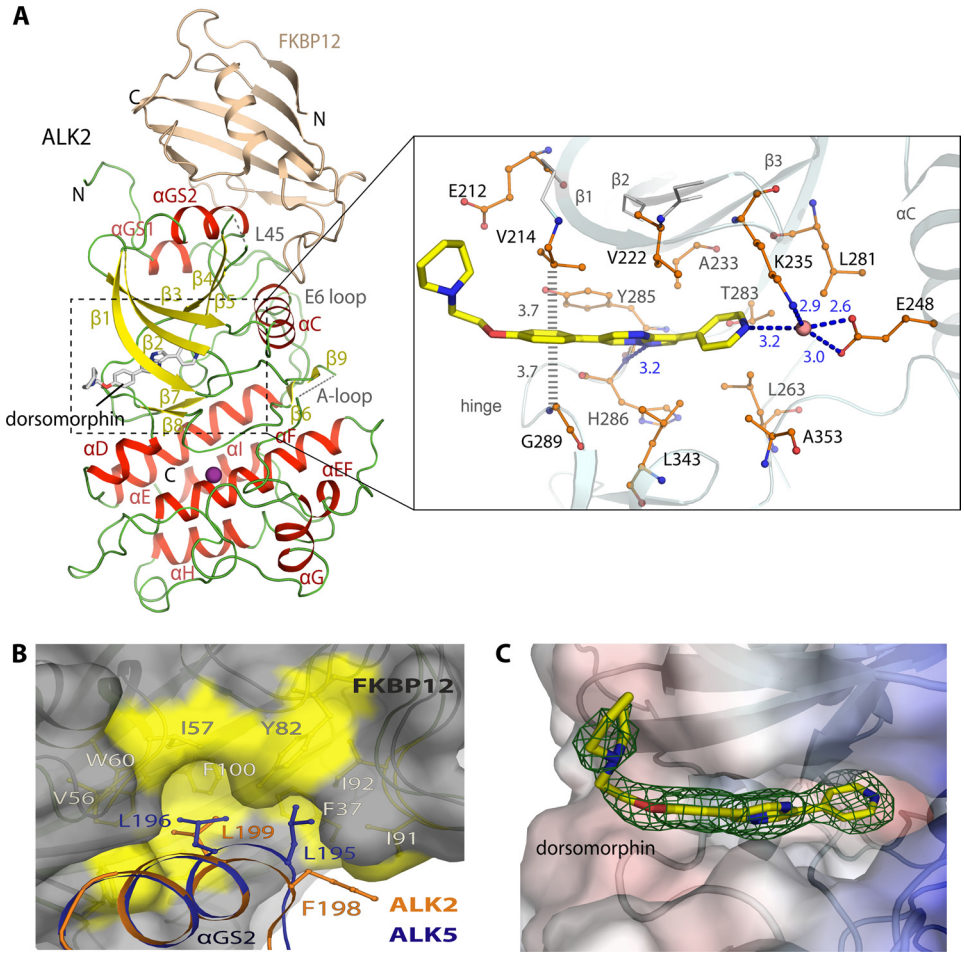

FIGURE 3. **Structure of the ALK2-FKBP12 complex.** *A*, secondary structure elements are labeled and shown as *ribbons*. Disordered parts of the L45 loop and A loop are indicated by a *thin dashed line*. Dorsomorphin is shown in *gray stick* representation, and Mg^{2+} ion (*cyan*) and sulfate molecules (*purple*) are displayed as *spheres*. *Inset box* shows the specific interactions of dorsomorphin (*yellow sticks*) with the ATP pocket in ALK2. Hydrogen bonds (*blue dashed lines*) are formed with the hinge amide of His-286 and via a water molecule to Glu-248 (αC). The planarity of the phenyl ring is restricted by the close packing of Val-214 and Gly-289 (*dashed gray lines*). *B*, FKBP12 binding is dominated by insertion of the αGS2 helix into the central FK506-binding pocket of FKBP12. Here, the ALK5 residues Leu-195–Leu-196 are replaced by ALK2 Phe-198–Leu-199 resulting in a subtle shift in the complex interface. The hydrophobic contact surface in FKBP12 is colored *yellow*. *C*, $|F_o| - |F_c|$ omit map contoured at 3σ (*green mesh*) for the bound dorsomorphin ligand (*yellow sticks*).

TABLE 1
Data collection and refinement statistics

	ALK2-FKBP12-dorsomorphin
PDB code	3H9R
Ligand	Dorsomorphin
Space group	$P2_12_12_1$
Cell dimensions	$a = 43.4$, $b = 62.4$, $c = 171.6$ Å $\alpha, \beta, \gamma = 90.0°$
Data collection	
Resolution[a]	42.15 to 2.35 Å (2.35–2.48 Å)
Unique reflections[a]	20,161 (2,892)
Completeness[a]	99.8% (100%)
Redundancy[a]	4.1 (4.0)
R_{merge}[a]	16.0% (68.4%)
$I/\sigma I$[a]	7.4 (2.0)
Refinement	
Resolution range	42.15 to 2.35
R_{fact}/R_{free}	18.7/25.6%
Atoms (protein/other)	3303/357
B-factors (protein/ligand)	24/22 Å^2
Root mean square deviation bonds	0.015 Å
Root mean square deviation angles	1.5°
Ramachandran[b]	
Favored	97.6%
Allowed	100%

[a] Values in parentheses represent statistics for highest resolution shells.
[b] Molprobity server analysis can be found on line.

4*C*). Both aspartates are critically required in all kinases for Mg-ATP binding and catalysis. ATP binding to ALK2 is further inhibited by an inactive conformation of the phosphate-binding loop (P loop) residue Tyr-219 (Fig. 4*C*).

FOP Mutations Destabilize the Inactive State—The ALK2 structure offers molecular explanations for the individual FOP mutations. Overall, the mutations are tightly clustered around the GS domain and ATP pocket (Fig. 5*A*). As shown in Fig. 4, in the wild-type structure these residues make critical interactions that stabilize the inactive state. FOP mutations are predicted to break these inhibitory interactions promoting a shift toward the active state.

The αGS2 helix forms a mutation hot spot and harbors the most frequent FOP mutation R206H alongside the mutations R202I and Q207E (Fig. 5*B*). All three residues bind the GS domain to the kinase N-lobe and form peripheral interactions that stabilize the inhibitory complex with FKBP12. Gln-207 forms hydrogen bonds with ALK2 Trp-227 (kinase domain β2) as well as Glu-55 in FKBP12 (Fig. 5*B*). In the Q207E FOP mutant, the juxtaposition of Glu-207 and Glu-55 would create electrostatic repulsion and weaken FKBP12 binding. Similar repulsion is expected in the caALK2 mutant Q207D. On the

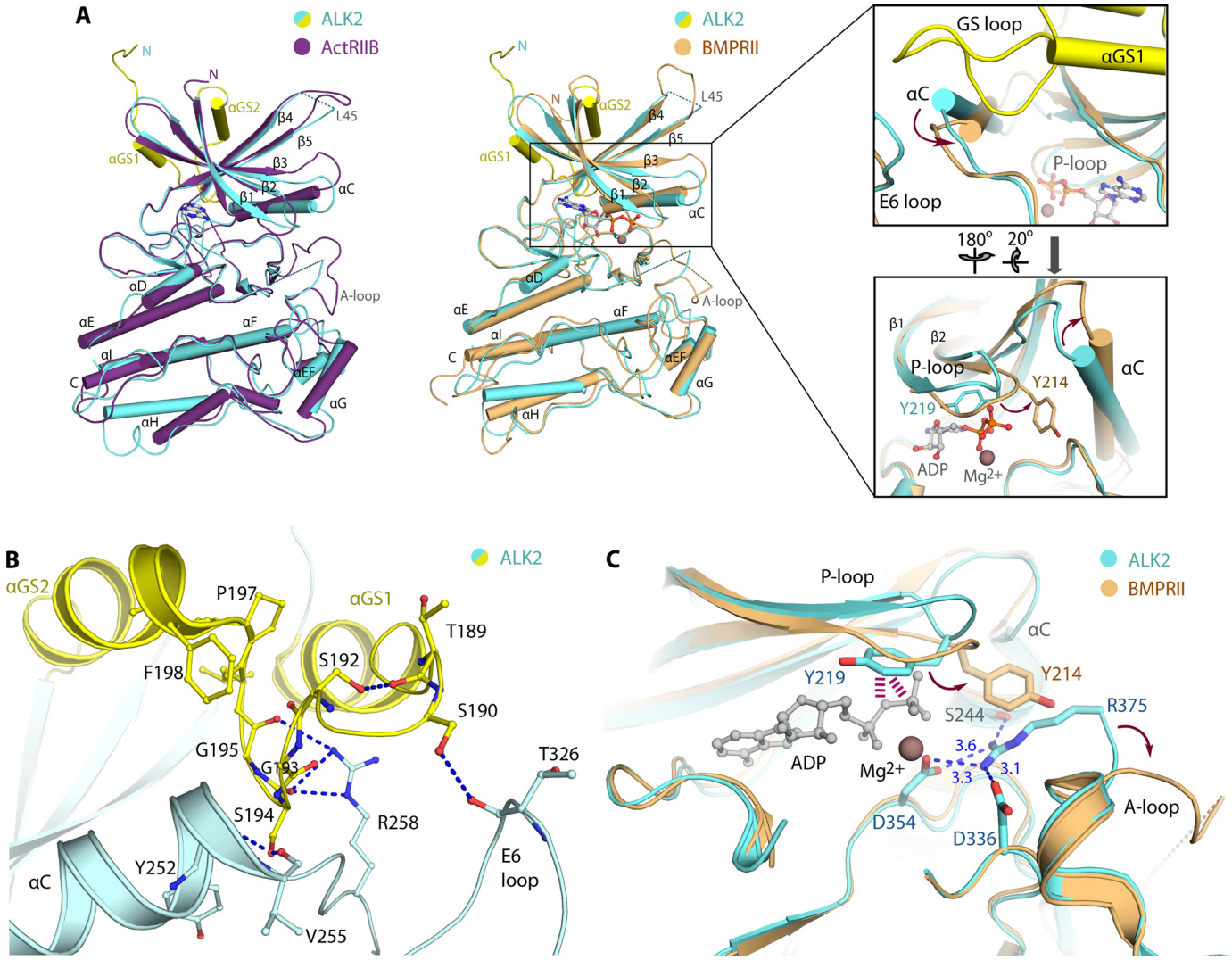

FIGURE 4. **Structural changes required for ALK2 activation.** *A*, ALK2 (*cyan*, kinase; *yellow*, GS domain) adopts an inactive structure as shown by superposition with the type II BMP receptors ActRIIB (*purple*; Protein Data Bank 2QLU) or BMPRII (*orange*; Protein Data Bank 3G2F). *Inset boxes* and *arrows* highlight the movements required for activation of ALK2 (back view, *top*; front view, *bottom*). *B*, specific side chain interactions from the *top inset box* in *A* are shown. Here, the ALK2 GS loop adopts a buried conformation that is stabilized by interaction with Arg-258. *C*, specific side chain interactions from the *lower inset box* in *A* are shown. Here, ATP binding is sterically inhibited in ALK2 by the conformations of Tyr-219 (P loop) and Arg-375 (A loop).

other face of the αGS2 helix, Arg-202 and Arg-206 form hydrogen bonds with Asp-269 (kinase domain β4), and Arg-206 forms a further hydrogen bond with the backbone oxygen of Met-270 (Fig. 5*B*). FOP mutations at these positions would break these bonds and destabilize the GS domain interactions with FKBP12 as well as the kinase L45 loop (Fig. 5*C*).

At the opposite end of αGS2, a deletion in FOP replaces Pro-197/Phe-198 with a single leucine residue, removing part of the FKBP12 interaction shown in Fig. 3*B*. Together with L196P, R258S, and G328R/G328W/G328E, this forms a mutation cluster bordering the buried GS loop. The P197_F198delinsL substitution would dramatically destabilize the inhibitory packing shown in Fig. 4*B*. Leu-196 is packed against the kinase β4 strand in the hydrophobic core of the GS domain (Fig. 5*C*). Arg-258 forms three hydrogen bonds to the GS loop. Gly-328 is located inside the neighboring E6 loop where no other side chain can be accommodated (Fig. 5*C*). Mutations at all three sites break critical bonds, providing freedom for the GS loop to move away from the kinase N-lobe, promoting an active kinase conformation. The remaining mutations G356D (DFG motif) and R375P (A loop) destabilize the inhibitory A loop conformation described in Fig. 4*C* resulting again in activation of ALK2. Until recently, the glycine position of the DFG motif was considered essential and invariant, but larger residues at this position have recently been identified in active kinases, including Haspin, and are well tolerated (46). In fact, G356D was the most active mutant in the presence of FK506, demonstrating the significant additive effects of structural changes in both the kinase and GS domains.

DISCUSSION

Here, we used a large panel of ALK2 constructs to show that weak gain of function is a common and specific disease feature shared by all FOP mutants. This was evidenced by leaky activation in the absence of ligand as well as an enhanced BRE-luciferase response to BMP4 and BMP6. Overall, mild constitutive activation was higher for GS domain mutants than those in the kinase domain. We demonstrated that the low basal signaling of FOP mutants was partly restricted by endogenous FKBP12. Thus, the

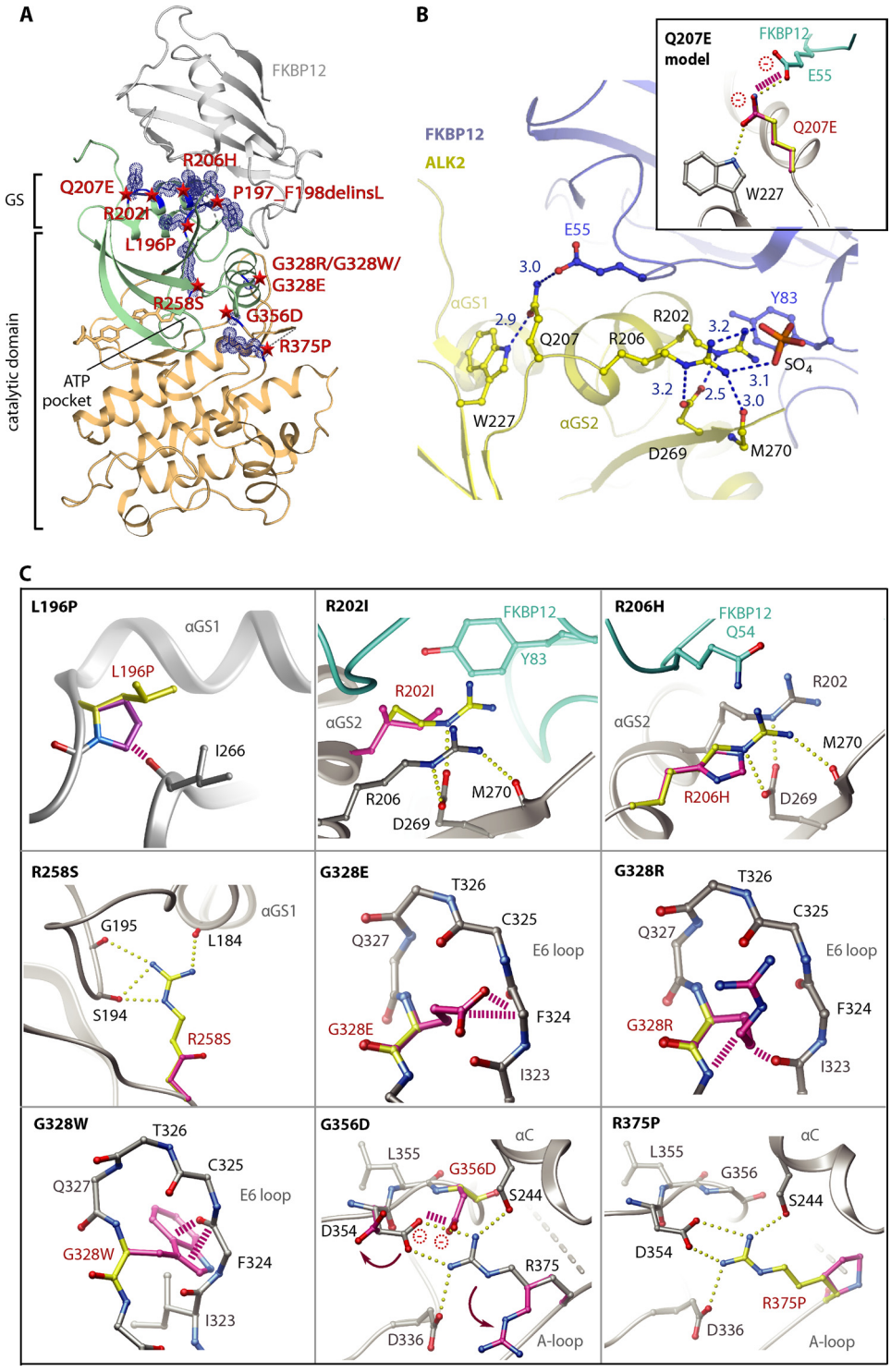

FIGURE 5. **FOP mutations destabilize the inactive state.** *A*, FOP mutation sites are clustered around the regulatory GS domain and ATP pocket. *B*, αGS2 helix in ALK2 is a hot spot for FOP mutation. *Inset* shows the likely charge repulsion between Q207E and FKBP12 Glu-55. *C*, structural models show that FOP mutations break inhibitory interactions in the ALK2-FKBP12 structure. Changes in the mutant structure are colored *purple* and overlaid onto the wild-type residue colored *yellow*. Hydrogen bonds in the wild type (*yellow*) and clashes in the mutant structure (*purple*) are shown by *spheres* and *dashed lines*, respectively. Models were generated using the Eris server (49).

full extent of mutant activation was only revealed upon displacement of FKBP12 with FK506. For the first time, this exposed the substantial gain of function inherent in many kinase domain mutants, including G356D.

The GS domain mutant L196P has raised particular interest for its association with a comparatively benign clinical course (18). In agreement with Ohte *et al.* (30), we found that the basal activity of L196P was surprisingly robust and similar to R206H. However, in contrast to R206H, the activity of L196P was not increased by FK506 and consequently fell below that of all other FOP mutants under this condition. The lower limit for constitutive L196P signaling in the absence of FKBP12 may offer one

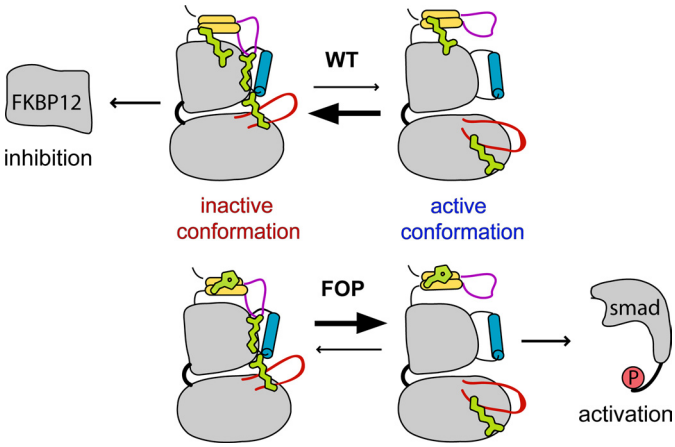

FIGURE 6. **Schematic for ALK2 activation in FOP.** The GS (*yellow*) and kinase (*gray*) domains are in equilibrium between inactive (*left*) and active (*right*) conformations. *Top,* in wild-type ALK2, FOP-associated residues (*green sticks*; Arg-206, Arg-258, and Arg-375) form critical interactions that maintain inhibitory conformations of the GS loop (*purple*), αC helix (*blue*), and A loop (*red*). The equilibrium is therefore shifted to the left, promoting binding of FKBP12. *Bottom,* in the R206H mutant, inhibitory GS-kinase domain interactions are broken, and the equilibrium is shifted to the right. FKBP12 is dissociated allowing interactions with the type II receptor (data not shown) (50). Opening of the GS loop and ATP pockets facilitates Smad assembly and phosphorylation.

explanation for a delayed onset of disease. In support of these data, we observed some binding of FKBP12 to R206H, whereas there was no binding to L196P. These data are consistent and complementary to previous BRE-luciferase assays using FKBP12 overexpression (28–30) as well as *in vitro* binding data (47).

FOP mutations have the potential to act through multiple (and overlapping) mechanisms, including changes to the kinase domain activation state and changes to the GS domain that diminish inhibition by FKBP12. A key observation from our study is that wild-type ALK2 signaling remains low even upon FK506 treatment. This suggests that FOP does not result from FKBP12 disruption alone. In agreement, Song *et al.* (28) showed that FK506 induced alkaline phosphatase staining in C2C12 cells stably expressing R206H but not wild-type ALK2. Together, these data support our assertion that FOP mutations act also to induce changes in the activation state of the catalytic domain. The observed level of constitutive activation is then modulated further by differences in FKBP12 affinity.

To understand the molecular basis for these effects, we solved the structure of the ALK2-FKBP12 complex. As observed for ALK5 (8, 9), FKBP12 functions not only to block access to the regulatory GS loop but also inhibits αC movements required for kinase activation. Our data show that the inactive conformation remains relatively stable in wild-type ALK2 even in the absence of FKBP12. Residues associated with FOP map exclusively to sites of structural change and form critical interactions to stabilize this inactive state. FOP mutations thus break bonds in the inhibited receptor that promote activation. The inactive conformation is therefore unstable in FOP mutant kinase domains, facilitating release of FKBP12 and activation of Smad (Fig. 6). This model agrees with earlier predictions for loss of autoinhibition (16) and offers a common mechanism to explain the action of all FOP mutations. The structure of the ternary ALK2-Smad complex remains to be determined and will be an important step to further rationalize the subtle differences between the artificial caALK2 mutant Q207D and the weaker FOP mutants such as Q207E.

In this study we define the structural changes between active and inactive BMP receptors and rationalize how this transition is compromised by FOP mutation. The structure of the ALK2-dorsomorphin complex also provides a new model for structure-based lead optimization of BMP inhibitors. Such inhibitors have many applications in cell signaling and stem cell biology and are proposed as potential therapeutics for heterotopic ossification as well as anemia of inflammation (48).

Acknowledgments—We thank Kirsten Petrie and Binesh Shrestra for help with ALK2 expression and staff at the Diamond Light Source for help with diffraction data collection. The Structural Genomics Consortium is a registered charity (number 1097737) that receives funds from the Canadian Institutes for Health Research, Genome Canada, GlaxoSmithKline, Lilly Canada, the Novartis Research Foundation, Pfizer, Takeda, AbbVie, the Canada Foundation for Innovation, the Ontario Ministry of Economic Development and Innovation, and the Wellcome Trust Grant 092809/Z/10/Z.

REFERENCES

1. Shi, Y., and Massagué, J. (2003) Mechanisms of TGF-β signaling from cell membrane to the nucleus. *Cell* **113,** 685–700
2. Kitisin, K., Saha, T., Blake, T., Golestaneh, N., Deng, M., Kim, C., Tang, Y., Shetty, K., Mishra, B., and Mishra, L. (2007) TGF-βa signaling in development. *Sci. STKE* 2007, cm1
3. Wu, M. Y., and Hill, C. S. (2009) TGF-β superfamily signaling in embryonic development and homeostasis. *Dev. Cell* **16,** 329–343
4. Wrana, J. L., Attisano, L., Wieser, R., Ventura, F., and Massagué, J. (1994) Mechanism of activation of the TGF-β receptor. *Nature* **370,** 341–347
5. Heldin, C. H., Miyazono, K., and ten Dijke, P. (1997) TGF-β signaling from cell membrane to nucleus through SMAD proteins. *Nature* **390,** 465–471
6. Derynck, R., and Zhang, Y. E. (2003) Smad-dependent and Smad-independent pathways in TGF-β family signaling. *Nature* **425,** 577–584
7. Wang, T., Li, B. Y., Danielson, P. D., Shah, P. C., Rockwell, S., Lechleider, R. J., Martin, J., Manganaro, T., and Donahoe, P. K. (1996) The immunophilin FKBP12 functions as a common inhibitor of the TGF-β family type I receptors. *Cell* **86,** 435–444
8. Huse, M., Chen, Y. G., Massagué, J., and Kuriyan, J. (1999) Crystal structure of the cytoplasmic domain of the type I TGFβ receptor in complex with FKBP12. *Cell* **96,** 425–436
9. Huse, M., Muir, T. W., Xu, L., Chen, Y. G., Kuriyan, J., and Massagué, J. (2001) The TGFβ receptor activation process. An inhibitor- to substrate-binding switch. *Mol. Cell* **8,** 671–682
10. Qin, B. Y., Chacko, B. M., Lam, S. S., de Caestecker, M. P., Correia, J. J., and Lin, K. (2001) Structural basis of Smad1 activation by receptor kinase phosphorylation. *Mol. Cell* **8,** 1303–1312
11. Wu, J. W., Hu, M., Chai, J., Seoane, J., Huse, M., Li, C., Rigotti, D. J., Kyin, S., Muir, T. W., Fairman, R., Massagué, J., and Shi, Y. (2001) Crystal structure of a phosphorylated Smad2. Recognition of phosphoserine by the MH2 domain and insights on Smad function in TGF-β signaling. *Mol. Cell* **8,** 1277–1289
12. Kaplan, F. S., Fiori, J., de la Peña, L. S., Ahn, J., Billings, P. C., and Shore, E. M. (2006) Dysregulation of the BMP-4 signaling pathway in fibrodysplasia ossificans progressiva. *Ann. N.Y. Acad. Sci.* **1068,** 54–65
13. Shore, E. M., and Kaplan, F. S. (2010) Inherited human diseases of heterotopic bone formation. *Nat. Rev. Rheumatol.* **6,** 518–527
14. Shore, E. M., Xu, M., Feldman, G. J., Fenstermacher, D. A., Cho, T. J., Choi, I. H., Connor, J. M., Delai, P., Glaser, D. L., LeMerrer, M., Morhart, R., Rogers, J. G., Smith, R., Triffitt, J. T., Urtizberea, J. A., Zasloff, M., Brown, M. A., and Kaplan, F. S. (2006) A recurrent mutation in the BMP type I receptor ACVR1 causes inherited and sporadic fibrodysplasia ossificans progressiva. *Nat. Genet.* **38,** 525–527
15. Furuya, H., Ikezoe, K., Wang, L., Ohyagi, Y., Motomura, K., Fujii, N., Kira,

J., and Fukumaki, Y. (2008) A unique case of fibrodysplasia ossificans progressiva with an *ACVR1 mutation, G356D, other than the common mutation (R206H). Am. J. Med. Genet.* **146,** 459–463
16. Kaplan, F. S., Xu, M., Seemann, P., Connor, J. M., Glaser, D. L., Carroll, L., Delai, P., Fastnacht-Urban, E., Forman, S. J., Gillessen-Kaesbach, G., Hoover-Fong, J., Köster, B., Pauli, R. M., Reardon, W., Zaidi, S. A., Zasloff, M., Morhart, R., Mundlos, S., Groppe, J., and Shore, E. M. (2009) Classic and atypical fibrodysplasia ossificans progressiva (FOP) phenotypes are caused by mutations in the bone morphogenetic protein (BMP) type I receptor ACVR1. *Hum. Mutat.* **30,** 379–390
17. Petrie, K. A., Lee, W. H., Bullock, A. N., Pointon, J. J., Smith, R., Russell, R. G., Brown, M. A., Wordsworth, B. P., and Triffitt, J. T. (2009) Novel mutations in ACVR1 result in atypical features in two fibrodysplasia ossificans progressiva patients. *PloS ONE* **4,** e5005
18. Gregson, C. L., Hollingworth, P., Williams, M., Petrie, K. A., Bullock, A. N., Brown, M. A., Tobias, J. H., and Triffitt, J. T. (2011) A novel ACVR1 mutation in the glycine/serine-rich domain found in the most benign case of a fibrodysplasia ossificans progressiva variant reported to date. *Bone* **48,** 654–658
19. Bocciardi, R., Bordo, D., Di Duca, M., Di Rocco, M., and Ravazzolo, R. (2009) Mutational analysis of the *ACVR1* gene in Italian patients affected with fibrodysplasia ossificans progressiva. Confirmations and advancements. *Eur. J. Hum. Genet.* **17,** 311–318
20. Whyte, M. P., Wenkert, D., Demertzis, J. L., DiCarlo, E. F., Westenberg, E., and Mumm, S. (2012) Fibrodysplasia ossificans progressiva. Middle-age onset of heterotopic ossification from a unique missense mutation (c.974G → C, p.G325A) in ACVR1. *J. Bone Miner. Res.* **27,** 729–737
21. Kan, L., Hu, M., Gomes, W. A., and Kessler, J. A. (2004) Transgenic mice overexpressing BMP4 develop a fibrodysplasia ossificans progressiva (FOP)-like phenotype. *Am. J. Pathol.* **165,** 1107–1115
22. Yu, P. B., Deng, D. Y., Lai, C. S., Hong, C. C., Cuny, G. D., Bouxsein, M. L., Hong, D. W., McManus, P. M., Katagiri, T., Sachidanandan, C., Kamiya, N., Fukuda, T., Mishina, Y., Peterson, R. T., and Bloch, K. D. (2008) BMP type I receptor inhibition reduces heterotopic (corrected) ossification. *Nat. Med.* **14,** 1363–1369
23. Wieser, R., Wrana, J. L., and Massagué, J. (1995) GS domain mutations that constitutively activate TβR-I, the downstream signaling component in the TGF-β receptor complex. *EMBO J.* **14,** 2199–2208
24. Medici, D., Shore, E. M., Lounev, V. Y., Kaplan, F. S., Kalluri, R., and Olsen, B. R. (2010) Conversion of vascular endothelial cells into multipotent stem-like cells. *Nat. Med.* **16,** 1400–1406
25. Fukuda, T., Kanomata, K., Nojima, J., Kokabu, S., Akita, M., Ikebuchi, K., Jimi, E., Komori, T., Maruki, Y., Matsuoka, M., Miyazono, K., Nakayama, K., Nanba, A., Tomoda, H., Okazaki, Y., Ohtake, A., Oda, H., Owan, I., Yoda, T., Haga, N., Furuya, H., and Katagiri, T. (2008) A unique mutation of ALK2, G356D, found in a patient with fibrodysplasia ossificans progressiva is a moderately activated BMP type I receptor. *Biochem. Biophys. Res. Commun.* **377,** 905–909
26. Fukuda, T., Kohda, M., Kanomata, K., Nojima, J., Nakamura, A., Kamizono, J., Noguchi, Y., Iwakiri, K., Kondo, T., Kurose, J., Endo, K., Awakura, T., Fukushi, J., Nakashima, Y., Chiyonobu, T., Kawara, A., Nishida, Y., Wada, I., Akita, M., Komori, T., Nakayama, K., Nanba, A., Maruki, Y., Yoda, T., Tomoda, H., Yu, P. B., Shore, E. M., Kaplan, F. S., Miyazono, K., and Matsuoka, M., Ikebuchi, K., Ohtake, A., Oda, H., Jimi, E., Owan, I., Okazaki, Y., and Katagiri, T. (2009) Constitutively activated ALK2 and increased SMAD1/5 cooperatively induce bone morphogenetic protein signaling in fibrodysplasia ossificans progressiva. *J. Biol. Chem.* **284,** 7149–7156
27. Shen, Q., Little, S. C., Xu, M., Haupt, J., Ast, C., Katagiri, T., Mundlos, S., Seemann, P., Kaplan, F. S., Mullins, M. C., and Shore, E. M. (2009) The fibrodysplasia ossificans progressiva R206H ACVR1 mutation activates BMP-independent chondrogenesis and zebrafish embryo ventralization. *J. Clin. Invest.* **119,** 3462–3472
28. Song, G. A., Kim, H. J., Woo, K. M., Baek, J. H., Kim, G. S., Choi, J. Y., and Ryoo, H. M. (2010) Molecular consequences of the ACVR1(R206H) mutation of fibrodysplasia ossificans progressiva. *J. Biol. Chem.* **285,** 22542–22553
29. van Dinther, M., Visser, N., de Gorter, D. J., Doorn, J., Goumans, M. J., de Boer, J., and ten Dijke, P. (2010) ALK2 R206H mutation linked to fibrodysplasia ossificans progressiva confers constitutive activity to the BMP type I receptor and sensitizes mesenchymal cells to BMP-induced osteoblast differentiation and bone formation. *J. Bone Miner. Res.* **25,** 1208–1215
30. Ohte, S., Shin, M., Sasanuma, H., Yoneyama, K., Akita, M., Ikebuchi, K., Jimi, E., Maruki, Y., Matsuoka, M., Namba, A., Tomoda, H., Okazaki, Y., Ohtake, A., Oda, H., Owan, I., Yoda, T., Furuya, H., Kamizono, J., Kitoh, H., Nakashima, Y., Susami, T., Haga, N., Komori, T., and Katagiri, T. (2011) A novel mutation of ALK2, L196P, found in the most benign case of fibrodysplasia ossificans progressiva activates BMP-specific intracellular signaling equivalent to a typical mutation, R206H. *Biochem. Biophys. Res. Commun.* **407,** 213–218
31. Yu, P. B., Hong, C. C., Sachidanandan, C., Babitt, J. L., Deng, D. Y., Hoyng, S. A., Lin, H. Y., Bloch, K. D., and Peterson, R. T. (2008) Dorsomorphin inhibits BMP signals required for embryogenesis and iron metabolism. *Nat. Chem. Biol.* **4,** 33–41
32. Leslie, A. G. (2006) The integration of macromolecular diffraction data. *Acta Crystallogr. D Biol. Crystallogr.* **62,** 48–57
33. Evans, P. (2006) Scaling and assessment of data quality. *Acta Crystallogr. D Biol. Crystallogr.* **62,** 72–82
34. McCoy, A. J., Grosse-Kunstleve, R. W., Adams, P. D., Winn, M. D., Storoni, L. C., and Read, R. J. (2007) Phaser crystallographic software. *J. Appl. Crystallogr.* **40,** 658–674
35. Cowtan, K., and Main, P. (1998) Miscellaneous algorithms for density modification. *Acta Crystallogr. D Biol. Crystallogr.* **54,** 487–493
36. Perrakis, A., Harkiolaki, M., Wilson, K. S., and Lamzin, V. S. (2001) ARP/wARP and molecular replacement. *Acta Crystallogr. D Biol. Crystallogr.* **57,** 1445–1450
37. Cowtan, K. (2006) The Buccaneer software for automated model building. 1. Tracing protein chains. *Acta Crystallogr. D Biol. Crystallogr.* **62,** 1002–1011
38. Murshudov, G. N., Vagin, A. A., and Dodson, E. J. (1997) Refinement of macromolecular structures by the maximum-likelihood method. *Acta Crystallogr. D Biol. Crystallogr.* **53,** 240–255
39. Emsley, P., and Cowtan, K. (2004) Coot. Model-building tools for molecular graphics. *Acta Crystallogr. D Biol. Crystallogr.* **60,** 2126–2132
40. Painter, J., and Merritt, E. A. (2006) Optimal description of a protein structure in terms of multiple groups undergoing TLS motion. *Acta Crystallogr. D Biol. Crystallogr.* **62,** 439–450
41. Davis, I. W., Leaver-Fay, A., Chen, V. B., Block, J. N., Kapral, G. J., Wang, X., Murray, L. W., Arendall, W. B., 3rd, Snoeyink, J., Richardson, J. S., and Richardson, D. C. (2007) MolProbity. All-atom contacts and structure validation for proteins and nucleic acids. *Nucleic Acids Res.* **35,** W375–W383
42. Mueller, T. D., and Nickel, J. (2012) Promiscuity and specificity in BMP receptor activation. *FEBS Lett.* **586,** 1846–1859
43. Lavery, K., Swain, P., Falb, D., and Alaoui-Ismaili, M. H. (2008) BMP-2/4 and BMP-6/7 differentially utilize cell surface receptors to induce osteoblastic differentiation of human bone marrow-derived mesenchymal stem cells. *J. Biol. Chem.* **283,** 20948–20958
44. Wang, T., Donahoe, P. K., and Zervos, A. S. (1994) Specific interaction of type I receptors of the TGF-β family with the immunophilin FKBP-12. *Science* **265,** 674–676
45. Han, S., Loulakis, P., Griffor, M., and Xie, Z. (2007) Crystal structure of activin receptor type IIB kinase domain from human at 2.0 Angstrom resolution. *Protein Sci.* **16,** 2272–2277
46. Eswaran, J., Patnaik, D., Filippakopoulos, P., Wang, F., Stein, R. L., Murray, J. W., Higgins, J. M., and Knapp, S. (2009) Structure and functional characterization of the atypical human kinase haspin. *Proc. Natl. Acad. Sci. U.S.A.* **106,** 20198–20203
47. Groppe, J. C., Wu, J., Shore, E. M., and Kaplan, F. S. (2011) *In vitro* analyses of the dysregulated R206H ALK2 kinase-FKBP12 interaction associated with heterotopic ossification in FOP. *Cells Tissues Organs* **194,** 291–295
48. Hong, C. C., and Yu, P. B. (2009) Applications of small molecule BMP inhibitors in physiology and disease. *Cytokine Growth Factor Rev.* **20,** 409–418
49. Yin, S., Ding, F., and Dokholyan, N. V. (2007) Eris. An automated estimator of protein stability. *Nat. Methods* **4,** 466–467
50. Le, V. Q., and Wharton, K. A. (2012) Hyperactive BMP signaling induced by ALK2(R206H) requires type II receptor function in a *Drosophila* model for classic fibrodysplasia ossificans progressiva. *Dev. Dyn.* **241,** 200–214
51. Korchynskyi, O., and ten Dijke, P. (2002) Identification and functional characterization of distinct critically important bone morphogenetic protein-specific response elements in the Id1 promoter. *J. Biol. Chem.* **277,** 4883–4891